SAE AERO DESIGN REPORT

Northern Arizona University

Skyjacks Team 045:
Caleb Hatcher
Damian Lumm
Angel Montiel
James Seganti
Braden Weiler

2018-2019

Statement of Compliance

APPENDIX A

STATEMENT OF COMPLIANCE

Certification of Qualification

Team Name: Team SkyJacks Team Number: 045

School: Northern Arizona University

Faculty Advisor: John Tester

Faculty Advisor's Email: John.Tester@nau.edu

Statement of Compliance

As faculty Adviser:

JT (Initial) I certify that the registered team members are enrolled in collegiate courses.

JT (Initial) I certify that this team has designed and constructed the radio controlled aircraft in the past nine (9) months with the intention to use this radio controlled aircraft in the 2019 SAE Aero Design competition, without direct assistance from professional engineers, R/C model experts, and/or related professionals.

JT (Initial) I certify that this year's Design Report has original content written by members of this year's team.

JT (Initial) I certify that all reused content have been properly referenced and is in compliance with the University's plagiarism and reuse policies.

John D. Tester
Signature of Faculty Advisor

James Bogyanti
Signature of Team Captain

Note: A copy of this statement needs to be included in your Design Report as page 2 (Reference Section 4.3)

Table of Contents

List of Figures and Tables

1.0 Executive Summary

The purpose of this report is to document the progress of the design and manufacturing of a fixed wing aircraft for the 2019 Society of Automotive Engineers (SAE) Aero Design West competition. Specifically, the report will layout the design process, the overall analysis of performance, testing and integration, and the manufacturing processes used. The design section of the report will include details about the optimization of the aircraft through multiple iterations of design that aimed to improve performance and scoring. Furthermore, reasoning for the selection of the dimensions and ratios from the Cessna 172 for the subassemblies will be described. Methods for analyzing the performance of the aircraft included finite element analysis, computational fluid dynamics, MATLAB programming, and excel worksheets. Through these methods the team ensured that the aircraft would be able to achieve the objectives of the competition with the goal in mind of maximizing scoring and competitiveness. The analyses described in this report have shown that the aircraft should be capable of flying and effectively completing the objectives of the competition. Furthermore, through finite element analysis the team has proved that the major structural members of the aircraft should hold up to the forces exerted on the system. For the testing of the aircraft, multiple flight sessions were used before the competition in order to adjust the design. Overall, by attending this competition it provides recognition for Northern Arizona University and the abilities of the students associated with this project.

1.1. System Overview

The aircraft designed by the team is based off the Cessna 172 [5] as the overall design contains similar features to those on the Cessna. Furthermore, the team's aircraft follows comparable ratios and dimensions from the Cessna since the design seemed to match general rules of thumb for aircraft design. By using the Cessna design as a template, the team was able to come up with a general design that was then modified to improve aspects such as weight, performance, and scoring. Along with that, the CH 10 airfoil [7] was selected for the main wing to maximize the lift of the aircraft with an angle of attack of zero degrees. The main structure of the aircraft lies within the aluminum spar that passes through the fuselage and is used for connection points for the tail and wing. Displayed below in Figure 1 is the final design of the aircraft.

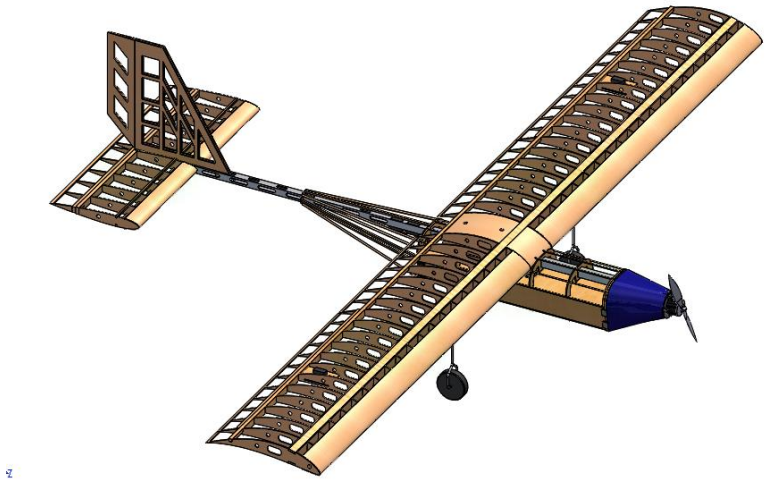

Figure 1: Team Skyjacks' final design

2.0 Schedule Summary

The team followed a strict schedule created in September at the beginning of the project. The schedule allowed for a significant amount of time to be allocated to in-depth analysis and design iterations based on the analysis. Through analyzing the failures of past year's teams and following the schedule, team Skyjacks was able to successfully design an airplane.

3.0 Table of Referenced Documents, References, and Specifications

Table 1: Referenced Documents, References, and Specifications

Reference	Specifications
[1] Staples, G. (2018). *Propeller Static & Dynamic Thrust Calculation - Part 1 of 2*. [online] Electricrcaircraftguy.com. Available at: https://www.electricrcaircraftguy.com/2013/09/propeller-static-dynamic-thrust-equation.html [Accessed 7 Nov. 2018].	Propeller static and dynamic thrust equations
[2] Staples, G. (2018). *Propeller Static & Dynamic Thrust Calculation - Part 2 of 2 - How Did I Come Up With This Equation?*. [online] Electricrcaircraftguy.com. Available at: https://www.electricrcaircraftguy.com/2014/04/propeller-static-dynamic-thrust-equation-background.html [Accessed 7 Nov. 2018].	Derivations of the propeller static and dynamic equations
[3] Tretta, F. (2018). *Tips for Manufacturing an RC Aircraft*.	Advice for design changes and manufacturing processes
[4] C. Gadd, "Servo Torque Calculator," Scale Flyers of Minnesota, [Online]. Available: http://www.mnbigbirds.com/Servo%20Torque%20Caculator.htm. [Accessed 18 February 2019].	Required servo torque equations and assumptions
[5] "Skyhawk: Model 172R - Specification & Description." Cessna: A Textron Company, Wichita, Mar-2011. Available at: https://web.archive.org/web/20110511100227/http://textron.vo.llnwd.net/o25/CES/cessna_aircraft_docs/single_engine/skyhawk/skyhawk_s&d.pdf	Dimensions, ratios, and data for the Cessna 172
[6] J. Anderson, *Fundamentals of Aerodynamics*, 6th ed. New York, NY: McGraw-Hill Education, 2017.	Rules of thumb for subassembly sizing and equations for analysis
[7] U. o. Illinois, "CH10 (Smoothed)," [Online]. Available: http://airfoiltools.com/airfoil/details?airfoil=ch10sm-il. [Accessed December 2018].	CH 10 airfoil data
[8] NeuMotors, "NeuMotors 4600 Series BLDC Motors," [Online]. Available: https://neumotors.com/neumotors-4600-series-bldc-motors-500-to-2000-watt-bldc-multicopter-motors/. [Accessed October 2018].	Specifications for the motor used on the aircraft
[9] Georgia State University, "Newton's First Law," Department of Physics and Astronomy, [Online]. Available: http://hyperphysics.phy-astr.gsu.edu/hbase/Newt.html. [Accessed February 2019].	Explanation and derivation of Newton's first law of motion
[10] U. o. Illinois, "NACA 0012 AIRFOILS (n0012-il)," [Online]. Available: http://airfoiltools.com/airfoil/details?airfoil=n0012-il. [Accessed December 2018].	NACA 0012 airfoil data
[11] https://www.cefns.nau.edu/Groups/fabricationShop/	NAU machine shop website

4.0 Design Layout & Trades

4.1. Overall Design Layout and Size

The final design of the aircraft is modeled after a Cessna 172 aircraft. A wingspan of 10 feet with a 1.3636-foot chord length is used and the length of the body is just under 7 feet, from tip to tail. The horizontal stabilizer has a wingspan of 2.725 feet and a chord length of 3.71 inches. The final weight of the plane is 15.81 pounds while unloaded and 28.29 pounds while loaded with the complete payload. Furthermore, the main structural support system for the aircraft is a square tubing aluminum beam which connects to the main wing, the fuselage bulkheads, and vertical and horizontal stabilizers. To secure the wing, it is bolted to the aluminum spar through a large balsa connection block that matches the profile of our wing's airfoil. All fuselage bulkheads have a square hole that the aluminum spar runs through, which gives the fuselage its main structural integrity. Between the bulkheads, the payload plates are vertically attached to the aluminum spar via bolts and nuts. The powertrain was set up based on the provided competition specifications, using an 18x8 propeller and a 4625 brushless electric motor. The tail that was chosen for the plane was a conventional design composed of a single horizontal and vertical stabilizers. The elevator used in the horizontal stabilizer was made from one single piece rather than two to simplify circuitry. The "passenger" tennis balls sit in a separate compartment in the bottom of the fuselage, which does not share a space with the payload plates. This compartment is approximately 6 inches underneath the aluminum bar. All aircraft components will be attached to the aluminum bar because it is the strongest structural component of the plane. Lastly, a "Taildragger" landing gear was chosen for the final design to accommodate the center of gravity's balance.

4.2 Competitive Scoring and Strategy Analysis

To score the maximum amount of points during the competition, the team optimized the amount of weight that our plane can carry. Twenty passengers will fit into the aircraft and an additional ten pounds in luggage, which combines for a total of 12.48 pounds of payload. In addition to this large payload, the team's strategy includes attempting to complete two full flights during the allotted 5-minute time period.

5.0 Loads and Environments, Assumptions

5.1. Design Loads Derivations

During the operation of the aircraft, the plane will experience several forces, accelerations, and impacts. The largest loads the aircraft will encounter that are likely to cause material failure are the impact forces from landing shock and pressure forces on the main wing.

The landing gear on the plane allows for a controlled, safe and non-destructive way to bring the aircraft back down to the runway. Without this system, the plane would likely break every flight when attempting to land rendering the aircraft useless when multiple flights are required. The design of the landing gear gives the landing maneuver a suspension character as the aluminum legs bend under impact. Also, the wheels allow the plane to roll along the runway without damage to the rest of the plane. In the event of a hard landing the strength of the landing gear will be tested. To check the strength, the team conducted an FEA analysis in ANSYS software assuming the impact force. The impact force was calculated using the impulse equation derived from Newton's First Law [9].

$$F\Delta t=mv \tag{1}$$

The mass of the aircraft was taken as the weight of the SolidWorks model which was 28.29 pounds. Velocity was inputted as the vertical direction during impact which was assumed to be

5 mph to simulate a poor landing. The time in which the landing gear was in contact with the ground was 0.1 seconds which seemed reasonable since the wheels are filled with air and the legs of the landing gear bend on impact. The result of this calculation was an average force of 304 N. The team assumed this to be a slight overestimate of what will be encountered since the plane will hopefully impact at a vertical speed much less than 5 mph.

The wing provides lift for the aircraft which allows the plane to get airborne and causes structural forces in the plane while accelerating. The lift force from the wing was modeled in ANSYS FEA software to test the strength of the wing and fuselage. The wing must be able to withstand aerodynamic forces without yielding or breaking components of the aircraft. A pressure force was imposed along the length of the wing which was equivalent to the max theoretical lift of about 40 lb. The team decided to assume a worst-case scenario if the plane were to dive or bank exceptionally hard by adding a factor of safety of two. When computing the FEA operation a pressure of twice the expected lift force was used.

5.2. Environmental Considerations

When performing analysis and simulations, considerations of the environment in Van Nuys, California have been used since it is the location of the competition. Calculations and simulations have been assumed to be at sea level meaning the humidity is zero, pressure is 1 atmosphere, and the temperature is roughly 55 °F. Additionally, it is assumed that the conditions for flying are optimal meaning that there would be no head wind affecting the speed of the aircraft. However, with test flights being done at nearly 7,000 feet in Flagstaff, Arizona, the aircraft will be tested in conditions that are harsher than those expected at the competition. Therefore, the aircraft should be optimized to perform well at the conditions of the competition if it is able to handle the conditions in Flagstaff.

6.0 Analysis

6.1. Analysis Techniques

Experimental and theoretical techniques were used in the analyses of the final design of the aircraft. These techniques required multiple computer programs and software to yield accurate results that influenced the final design. These tools were used to analyze both the structural integrity and the performance of the plane. The tools that were used to conduct the theoretical techniques were Microsoft Excel, MATLAB, SolidWorks CAD, and ANSYS Workbench. All analyses were based on the 3D models that were created in SolidWorks, then the models were converted into different file types in order to be imported into other software for further analysis. Once materials were ordered and delivered, experimental tests were able to be completed. Performance and strength aspects of the design were put to the test using experimental methods to optimize dimensions and materials for certain parts of the aircraft. Both techniques positively benefited the design to create a competitive plane for competition.

6.2 Performance Analysis

6.2.1. Thrust Performance

To analyze the thrust performance of the design, team Skyjacks created a test to determine what propeller should be used with the 1000 W motor and 22.2 V battery which had already been purchased. The motor, battery, ESC, receiver, and transmitter were all set up and connected to a Turnigy Thrust Stand. This set up is shown in Figure 2. This thrust stand, when set up in the configuration shown, can measure the static thrust generated from a propeller connected to the motor. A variety of propellers were tested with different diameters and pitches. These results are shown in Table 2.

Table 2: Static thrust test results

Propeller	Static Thrust at Full Throttle (lb)
18x8	10.58
14x8	6.83
16x8 (B)	9.04
16x8 (G)	8.16
16x6	8.38
16x12	9.04

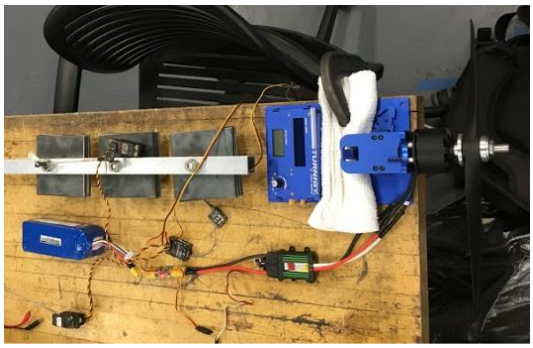

Figure 2: Thrust test setup

The team chose the 18x8 propeller in order to maximize the thrust produced at full throttle. With this setup, the battery life at full throttle was calculated to be approximately six minutes, enough time for the team to complete successful flights at the competition in the allotted two minutes.

Since the airplane will be moving at a specific velocity, to properly estimate the in-flight thrust, dynamic thrust must be estimated. This is estimating the effect the airplane's velocity has on the thrust the propeller produces. This estimation was done using an approximation developed by Gabriel Staples [1], a prominent RC aircraft enthusiast. Staples' method estimates dynamic thrust from static thrust and the properties of the propeller. Dynamic thrust was estimated to be linearly decreasing with an increase in velocity from the maximum measured static thrust to zero thrust at some velocity. This velocity is estimated to be equal to the pitch speed of the propeller [1]. From the static thrust test performed on the 18x8 propeller, assuming constant

RPM, the pitch speed was calculated to be 56.8 mph. From this dynamic thrust was estimated and plotted, the results can be seen in Figure 3.

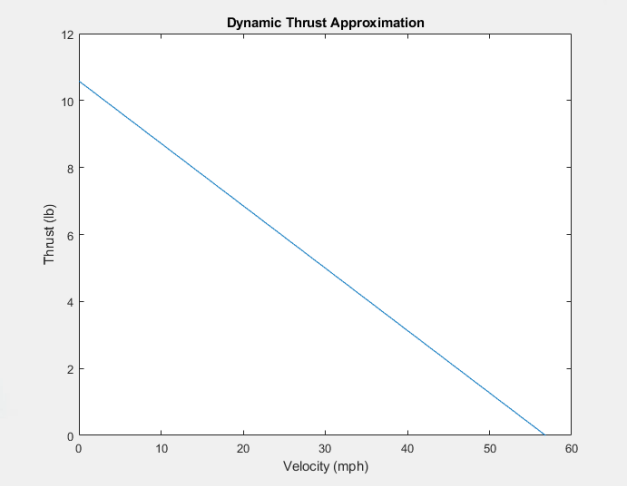

Figure 3: Dynamic thrust approximation for team Skyjacks' design

6.2.2. Drag Performance

To estimate the drag of the entire aircraft, the drag coefficient of each of the major components were calculated. These drag coefficients of components are shown in Table 3.

Table 3: Coefficients of drag for each of the major aircraft components

Component	Coefficient of Drag
Fuselage	0.82 [6]
Vertical Stabalizer	0.04 [6]
Landing Gear	0.47 [6]
Horizontal Stabalizer	0.01 [10]
Wing Sectional	0.0206 (see Appenix A, Figure 13)

To calculate the coefficients of drag for the entire airplane, the angle of attack was assumed to be zero. Eqn. 2 was used to calculate the coefficient of induced drag, $C_{D,i}$, of the wing [6].

$$C_{D,i} = \frac{C_L^2}{\pi AR}(1+\delta) \tag{2}$$

In Eqn. 2, δ is the induced drag factor found in Figure 14 in Appendix A from the wing aspect ratio and taper ratio while C_L is the coefficient of lift of the wing. From this the coefficient of induced drag of the wing was calculated to be 0.0644. By adding the coefficient of induced drag

to the wing's sectional coefficient of drag, c_d, the wing's coefficient of drag was found to be 0.0850 [6].

To solve for the total drag on the airplane, the actual drag of each component was calculated through Eqn. 3. In Eqn. 3 C_D is the coefficient of drag for each component, q_∞ is the freestream dynamic pressure, and A is the relevant area of the component [6].

$$D = C_D q_\infty A \tag{3}$$

The drag on each component was then added together for the total drag on the airplane. By leaving freestream velocity variable in this calculation, the airplane's total drag could be plotted with velocity as shown in Figure 4.

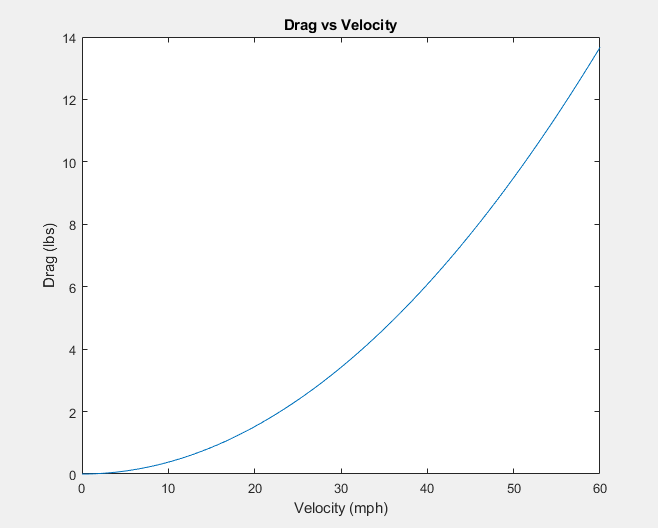

Figure 4: Plot of Drag vs Velocity for team Skyjacks' airplane

Drag and dynamic thrust are opposing forces on the same axes of the aircraft both varying with velocity. These forces are plotted in Figure 5.

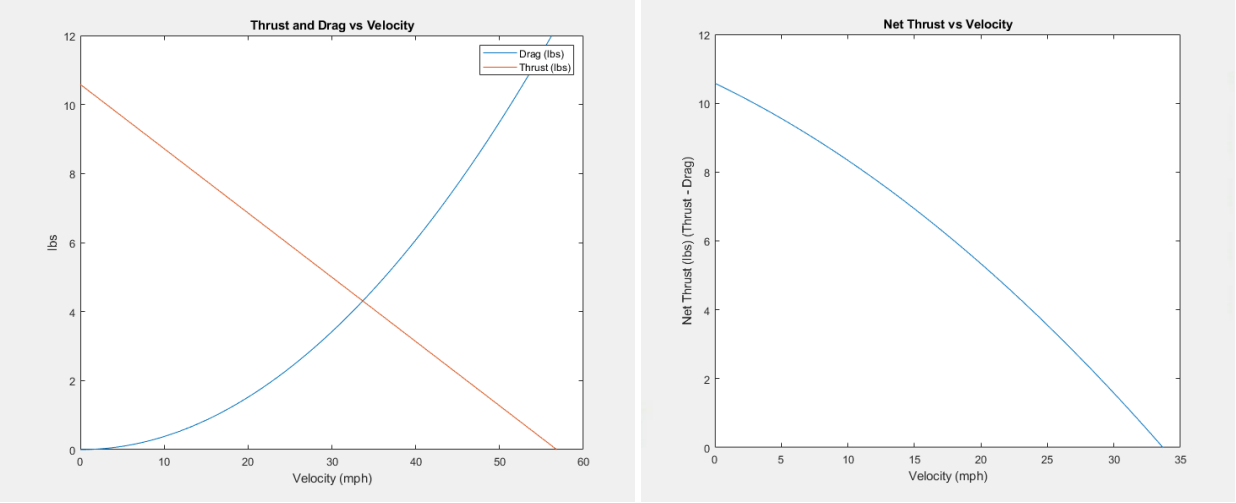

Figure 5: Plot of dynamic thrust and drag with changing velocity and plot of the aircraft's net thrust force with changing velocity

By subtracting the aircraft drag from the predicted dynamic thrust, a net thrust force was calculated and plotted in Figure 5. This information is important because when the net thrust is zero (that is when the aircraft thrust and drag are equal), the airplane has reached its terminal velocity.

6.2.3. Lift Performance

With the CH10 airfoil at zero angle of attack, the sectional coefficient of lift, c_l, is 1.175 (see Figure 13 of Appendix A) [7]. Because the wing design chosen is a constant airfoil, has a constant chord length, and a constant angle of attack the team chose to assume that, for analytical purposes, the wing is uniformly loaded and therefore the wing coefficient of lift, C_L, will be equal to the sectional coefficient of lift. From this, the lift on the wing is estimated using Eqn. 4., where S is the wing plan form area [6].

$$L = C_L q_\infty S \tag{4}$$

By leaving freestream velocity variable in this calculation, the aircraft's lift could be plotted with velocity as shown in Figure 6.

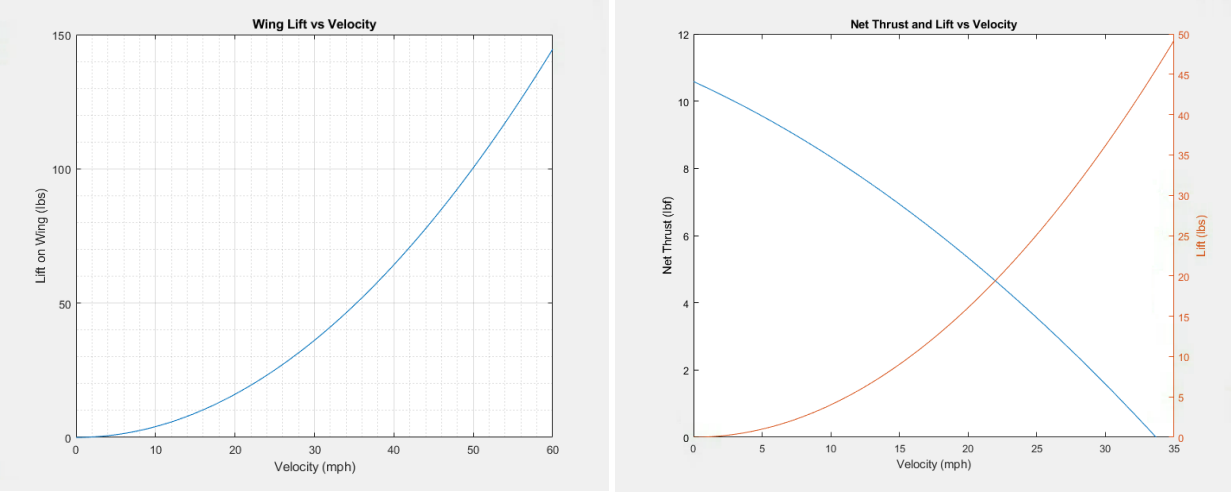

Figure 6: Plot of the airplane's lift vs velocity and plot showing the aircraft lift and net thrust at different velocities

To visualize the forces acting on the aircraft, Figure 6 was created to clearly show what the lift and net thrust will be on the airplane at different velocities.

6.2.4. Takeoff Performance

An essential part of the aircraft's performance is being able to take off and land successfully and safely. With a total aircraft weight of 28 lb, based on the lift analysis, the airplane will need a freestream velocity of 26.5 mph to have 28 lb of lift and therefore achieve liftoff.

Based on the competition rules, the aircraft must achieve liftoff in 200 feet or less. To verify that team Skyjacks' airplane was capable of this, the runway acceleration was estimated by Eqn. 5 where the net thrust force is variable with velocity as shown in Figure 5.

$$a_{runway} = \frac{T_{net}}{m_{total}} \tag{5}$$

In Eqn. 6, a_{runway} is the estimated runway acceleration, now as a function of velocity, T_{net} is the net thrust force, and m_{total} is the total aircraft mass. This acceleration assumes that the motor is already at full throttle from the starting line. Then to find the takeoff distance, the integral shown in Eqn. 6 was performed numerically. In Eqn. 6 s is the estimated distance to takeoff, and $v_{takeoff}$ is the approximated takeoff speed.

$$s = \int_0^{v_{takeoff}} \frac{v}{a_{runway}} dv \quad (6)$$

This calculation gave an estimated takeoff distance of 83.8 feet, safely within the 200 feet limit. This distance assumes that the aircraft is achieving its maximum possible thrust from the start line, so it is an underestimation. The estimation does not account for factors such as starting from no throttle and errors in the drag estimation.

6.2.5. Flight and Maneuver Performance

While in flight, the minimum freestream velocity the airplane must hold to avoid losing altitude is 26.5 mph. As shown in section 6.2.3 and section 6.2.4, this is the freestream velocity at which the airplane's lift is equal to its weight. The terminal velocity of the aircraft at zero angle of attack, when the drag force and thrust force are equal, is 33.6 mph. This is based on the analysis done to produce the plot in Figure 5 in section 6.2.2.

The aircraft utilizes a Spektrum AR6600T Six Channel receiver and a Spektrum DX6 transmitter to control the electronics. To ensure that the servos are sized appropriately for the ailerons, rudder, and elevator the following equation was implemented in a MATLAB program:

$$T = 8.5 * 10^{-6}\left(\frac{C^2V^2Lsin(s_1)+\tan(s_1)}{\tan(s_2)}\right) \quad (7)$$

In this equation, T is the required torque for the servo (oz-in), C is the average chord of the control surface (cm), V is the velocity of the aircraft (mph), L is the length of the control surface (cm), S_1 is the max control surface deflection, and S_2 is the max servo deflection [4]. In order to perform this calculation, an airspeed of 45 miles per hour was assumed which is in the case of a dive situation to ensure the servos can handle the maximum speeds of the aircraft. Furthermore, the maximum deflections of the control surface and servo arm are assumed to be 30 degrees and 45 degrees respectively as a conservative assumption. Through this equation,

the team calculated that the required servo torque for the ailerons, elevator, and rudder are 29.15 oz-in, 36.68 oz-in, and 20.84 oz-in respectively. These torque values should be able to handle any conditions that the aircraft encounters as a factor of safety is associated by using an airspeed over ten miles per hour faster than the expected speed. The servos that were purchased are rated at 130.53 oz-in at 6.0 volts which is considerably higher than needed, but there should be minimal chances of a failure.

6.2.7. Aeroelasticity

In order to analyze the aerodynamic forces imposed on the aircraft during flight, a Finite Element Analysis was completed on the main wing. While the plane is airborne there will be air pressure forces and gravity forces acting over the entire body. It is important to verify that the wing will maintain structural integrity and keep shape so that the plane creates constant lift and the aircraft remains controllable.

The Main wing was tested by applying an upward pressure force on the two main spars. The center connection block was held as a fixed support and a gravity force was applied to the entire model. This situation seen in Figure 7 imitates the uniform lifting force across the length of the wing. The loading from the air pressure force will not be uniform, but the constant cord design makes a uniform loading an appropriate estimation. Also, the model was altered slightly to allow for easier meshing in the ANSYS software, however, the important geometries were kept. The pressure applied to the model applies 80 lb of force on the wing which is double the expected loading during constant velocity level flight. This is to account for accelerations such as turns and dives that can cause a spiked force.

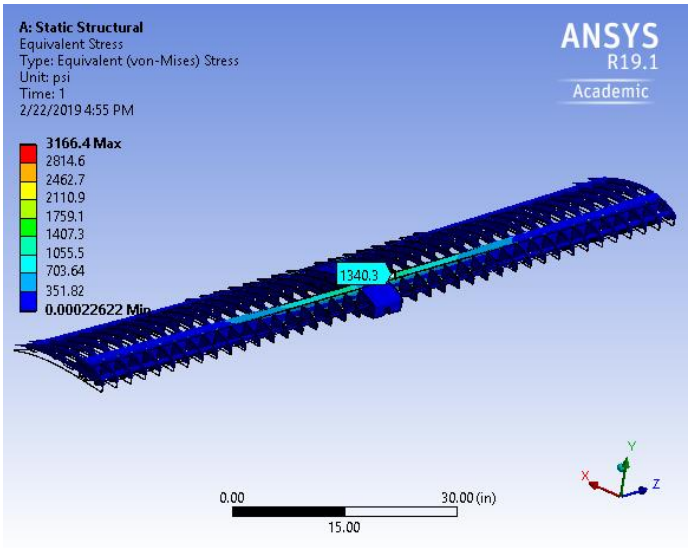

Yield Strength (psi)	Max Equivalent Stress (psi)	Max Deformation (in)
4730	1340.3	0.84

Figure 7: Contour Plot of Stress in Main Wing

The max stress occurs in the basswood cross member which has a yield stress of 4730 psi. Based on the results, there will not be any components that will break. It was also found that there were very low amounts of stress in the Balsa airfoils. Lastly, each side of the wing will bend up 0.84 in. This deformation is not a concern because it will not affect the lift performance significantly and there was no noticeable twisting along the length of the wing.

6.3. Structural Analysis

Structural integrity of the aircraft was analyzed using ANSYS Workbench FEA software. Three case studies were completed to analyze the structure of the aircraft, one on the aluminum spar, a second on the nose assembly attached to the aluminum spar, and a third study on the landing gear and the shock it creates on the main wing. Since the aluminum spar is the main structural support component of the aircraft, it will have many loads on it throughout the entire length of the beam. The spar with the nose assembly is where the main force that is propelling the aircraft is generated and if the nose assembly does not have the strength to pull the aircraft,

the design would have been flawed and inadequate. The landing gear is critical to the scoring strategy of attempting to land and complete two full flights, and a failure to the landing gear would be detrimental to the aircraft.

6.3.1. Applied Loads and Critical Margins Discussion

The aluminum spar was analyzed with a total of 7 axial loads and 2 moments. The forces and moments are due to 4 components that experience loads during flight: the main wing, the vertical stabilizer, the horizontal stabilizer and the payload. In addition to approximating the flight loads, it was assumed that the front of the spar is a fixed end, and therefore has boundary conditions of no movements in the x, y, or z direction. The main wing and horizontal stabilizer created moments about the z-axis of the beam, the rudder created an axial force in the x direction of the beam, and the payload created forces due to weight in the y-axis of the plane. All forces and moments on the spar are assumptions based on results from the servo analysis as well as the weight and location of our payload plates. Each force was given a factor of safety of two to analyze the plane under maximum flight conditions.

From the analysis, stresses and deformations in the beam were calculated. Figure 8 shows the contour plot of the stress in the beam, with the legend on the left-hand side of the figure. The highest stress points occur towards the FWD end of the beam with the highest stress in the beam being calculated at 2,778.2 psi. The yield stress of the beam is 40,611 psi so there are no concerns about the beam failing during flight. Deformation of the beam was largest in the AFT end of the plane due to the assumption that the nose was a fixed support. This makes the back end of the beam a large moment and causes the most deflection. The highest total deformation in the beam was 0.40483 inches, but again this is under the absolute worst-case scenario possible which, given that it is a 7-foot-long beam, is not of great concern during flight.

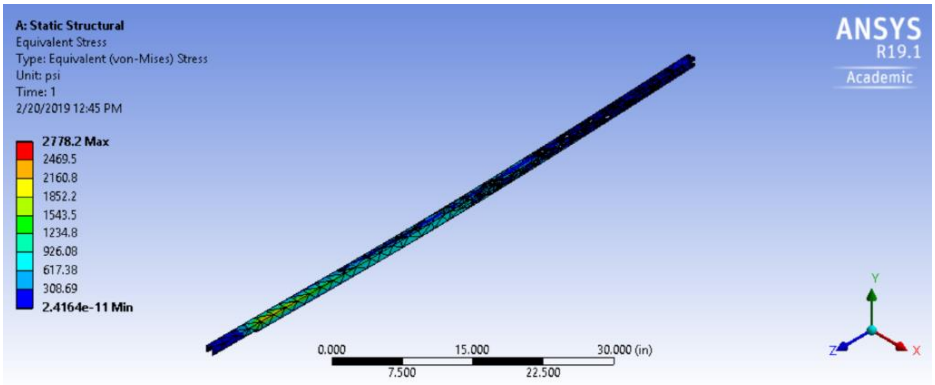

Figure 8: Contour Plot of Stress in Aluminum Spar Beam

The second Finite Element Method analysis was complete on the nose assembly in conjunction with the aluminum beam. Only one load, of 11.24 lbf, was placed on the motor shaft of the nose assembly. This is to simulate the force that the propeller will put on the nose assembly, refer to Figure 9. The force of 11.24 lbf was chosen because that is double the thrust force that the aircraft propeller and motor generate when tested with the Turnigy Thrust Stand. This is a crucial analysis because if the nose assembly is not strong enough to pull the full weight of the aircraft, then the design is flawed. Similarly, equivalent stress and total deformations were solved for the nose assembly. The maximum total stress in the beam is 1547.9 psi which is far from the yield stress of the assembly. The max total deformation of the nose and connecting pieces is 1.0593e-3 in, which is minimal compared to the overall size of the nose assembly.

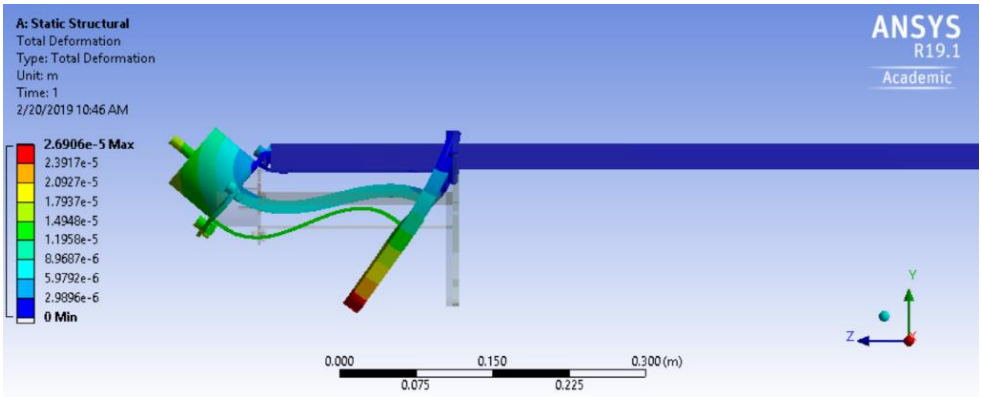

Figure 9: Contour Plot of Nose Assembly and Aluminum Spar Beam

The third Finite Element Method analysis was done on the landing gear because this component will experience high loads when the aircraft lands. Figure 10 below displays the applied force on the model which was 34.2 lb, this was calculated using Eqn. 1 and assuming the weight of the plane and a vertical landing speed of 5 mph. A 35 lb force was applied at the center of the wheel at an angle of 7.5° which is the angle the plane makes with the ground while at rest.

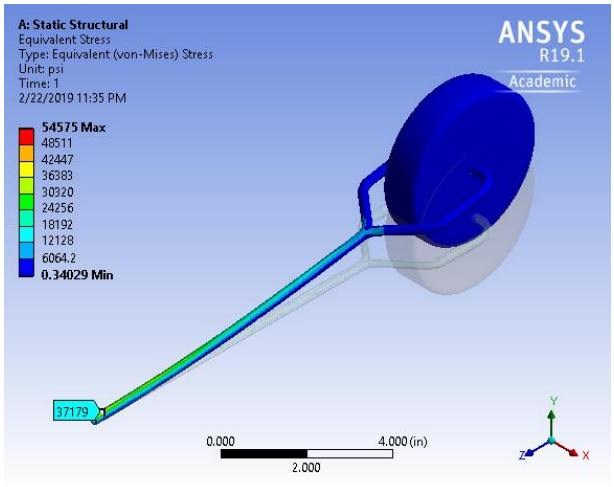

Yield Strength (psi)	Max Equivalent Stress (psi)	Max Deformation (in)
40611	37179	1.71

Figure 10: Contour Plot of Stress in Single Leg of Landing Gear

The results from this analysis show very high stresses in the shaft of the landing gear. The aluminum is very close to yielding and the wheel deflects 1.71in from its unloaded position. ANSYS also provides tabulated results for an aluminum S-N curve which says the aluminum will yield after about 5000 cycles of this loading due to fatigue. The team decided to use this design anyways because the material has already been ordered. If problems arise in the landing gear during test flights, the team will manufacture new landing gear with a bigger diameter shaft.

The impact from landing will also affect the wing since the landing gear is directly connected to the main wing. Figure 11 presents another analysis that was conducted on the wing in the event of an impact landing to view how stresses would translate to the wing. A 35 lb load was applied where the landing gear connects to the wing. The fixed support and gravity force were applied in the same way as the first FEA on the wing.

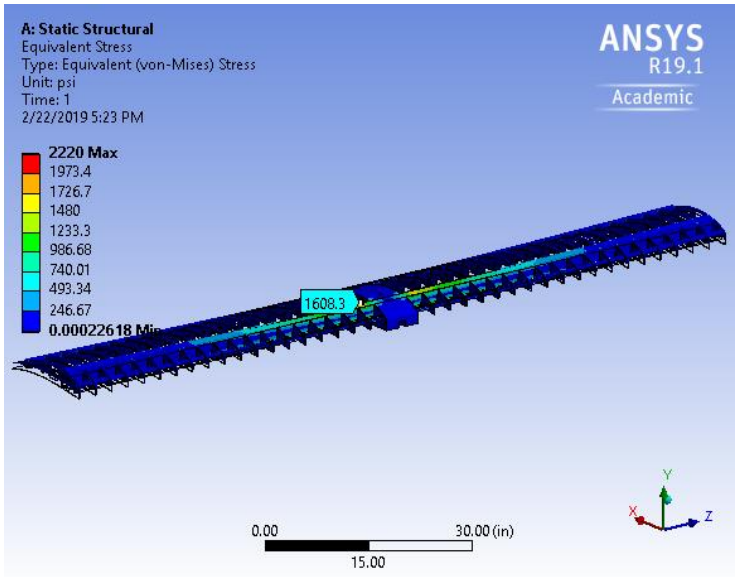

Yield Strength (psi)	Max Equivalent Stress (psi)	Max Deformation (in)
4730	1608.3	0.907

Figure 11: Contour Plot of Stress from the Landing Gear onto the Main Wing

The results show that the stresses in the wing are significantly less than the yield stress of Basswood which means there will not be any structural damage upon landing.

7.0 Assembly and Subassembly, Test and Integration

The first testing procedure that the team integrated into the design process of the aircraft was the static thrust tests using the as Turnigy Thrust Stand described in section 6.2.1. Another testing procedure the team has implemented is creating a simulation of our aircraft in the Real Flight simulator to see how the dimensions and ratios of our plane work as an overall system.

To create the model of the aircraft in the simulator, a plane with a comparable design is chosen and then the dimensions of the subassemblies can be changed to match the ones of the SolidWorks model. Before the plane is flown in the simulator the power generated is lowered to produce similar speeds that the team's aircraft should achieve. With the use of the simulator the team has verified that the aircraft should be able to take off and maintain flight and information about the controllability of the aircraft has been provided. An additional procedure the team will implement is a small scale lift and drag test verification of the CH 10 airfoil in a wind tunnel at the Northern Arizona University machine shop [11]. Figure 12 displays the team's test setup of the 3D printed airfoil in the wind tunnel.

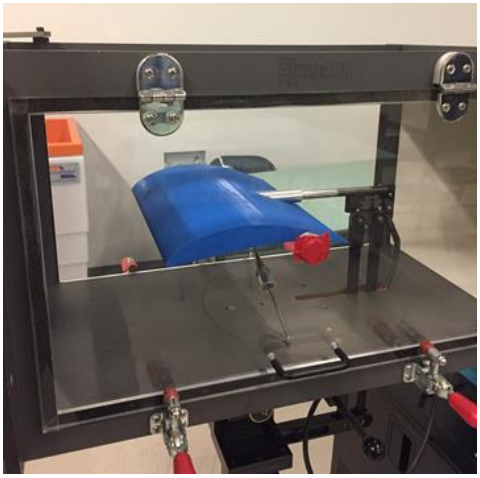

Figure 12: CH10 airfoil small scale wind tunnel test

After extensive testing of the subassemblies associated with the aircraft, the test of the full system will be done at a dry lake bed near Flagstaff, Arizona. The reason for choosing the dry lake bed is to provide a large flat area where the aircraft can be landed at any time and to minimize the obstacles the aircraft could encounter. With the testing being done at a higher elevation than the competition, it will be more difficult to fly, but if it can perform effectively at 7,000 feet then theoretically it should work better at sea level. Therefore, the test flights done

near Flagstaff will be challenging, but informative as well as it will provide enough evidence of whether the aircraft will perform as expected.

8.0 Manufacturing

Following the design, analysis, and testing of the plane, the team was able to bring the design to life with the building processes. The aircraft design requires a variety of manufacturing processes including laser cutting, sanding, gluing, and milling.

Laser cutting was one of the team's most crucial tools when manufacturing the plane because it allowed for very accurate and irregular geometries to be cut out of sheets of wood. The airfoils for the main wing and horizontal stabilizer required the precision offered by the laser cutter because they produce the shape of the control surfaces which allow for flight. The analysis executed for the design of the aircraft relies on the specific lift and drag coefficients produced by the CH-10 and NACA 0012 profiles. Other components of the plane composed of Balsa and Birch Plywood were also cut with the laser cutter despite not requiring the accuracy. These parts included the fuselage bulkheads, tennis ball carrier, vertical stabilizer, and other small components. The laser cutter was utilized on these parts as well due to the simplicity especially since all the components of the plane were modeled in SolidWorks and could easily be converted to a ".dxf" for laser cutting. Another reason for the extensive use of the laser cutter is the team's free access to the local high school's facilities.

Although most of the plane components made from wood were manufactured with the laser cutter, the assembly process includes further refinement. There are several components of the plane that are made from wood and are not able to be laser cut. These pieces, which included the bulkier spars and blocks, need to be cut and sanded manually. The CA glue used to connect

all the pieces together is a strong yet lightweight two-part epoxy. The tolerances set in the design of the aircraft, were made however knowing wood can be manipulated easily with sanding and bending. In addition, the grain of the wood while assembling was aligned in the same direction as any compressive or tensile forces for each piece.

The design also includes a significant amount of aluminum parts which were machined at the NAU machine shop and purchased through online metal merchants [11]. All the metal used on the plane was 6061 Aluminum which was implemented on the aircraft's landing gear, main fuselage spar, nose section, and hardware. The motor mount and landing gear bracket were modeled in SolidWorks and Autodesk Fusion 360 in order to generate 3-axis mill G-code to be run on a Tormach CNC. Other aluminum components did not require the same amount of accuracy and were manufactured using a manual mill, band saw, and sanders. The assembly of the nose and the landing gear required TIG welding while the aluminum spar and motor mount consisted of hardware connection points.

The purchased components of the aircraft included the wheels, propeller, servo system, and monokote. These items required little to no manufacturing as they only needed to be mounted to the plane. The propeller was mounted on the motor shaft with a prop adaptor and a safety nut. The servo assemblies for the control surfaces on the plane were glued into the main wing and aluminum spar. The wheels were attached to the landing gear with press fit bearings. Lastly, monokote was used to cover the aircraft allowing for pressure forces responsible for lift, which was shaped to the contours of the plane with a heating iron.

9.0 Conclusion

After multiple iterations in the design phase and different approaches for analysis and testing, Team Skyjacks is confident that the aircraft will complete all the objectives laid out by the competition. With a high lift airfoil, lightweight construction, and durable structural integrity, the aircraft should be successful and represent Northern Arizona University appropriately. While there have been setbacks and challenges throughout the project, the Skyjacks have overcome these through outside advice and skills learned at the university. Ultimately, the team believes that the aircraft reflects the hard work and countless hours that have been put in to represent the university in a positive manner and display the skills that have been learned throughout this project.

List of Symbols and Acronyms

F: Force
t: time
m: mass
v: velocity
$C_{d,i}$: coefficient of induced drag
C_L: total coefficient of lift
c_l :sectional coefficient of lift
AR: aspect ratio
δ: induced drag factor
C_D: total coefficient of drag
c_d: sectional coefficient of drag
L: Lift
D: Drag
q_∞: dynamic pressure
A: area
S: wing plan form area
a_{runway}: runway acceleration
T_{net}: net thrust
m_{total}: total aircraft mass
s: takeoff distance
$v_{takeoff}$: liftoff velocity
T: torque
C: control surface average chord
V: velocity
L: control surface length
s_1: max control surface deflection
s_2: max servo deflection
α: angle of attack
NAU: Northern Arizona University
RPM: Rotations per minute
CNC: Computer numerical control
c_t/c_r: taper ratio, wing tip chord/wing root chord

Appendix A – Figures Supporting Performance Analysis

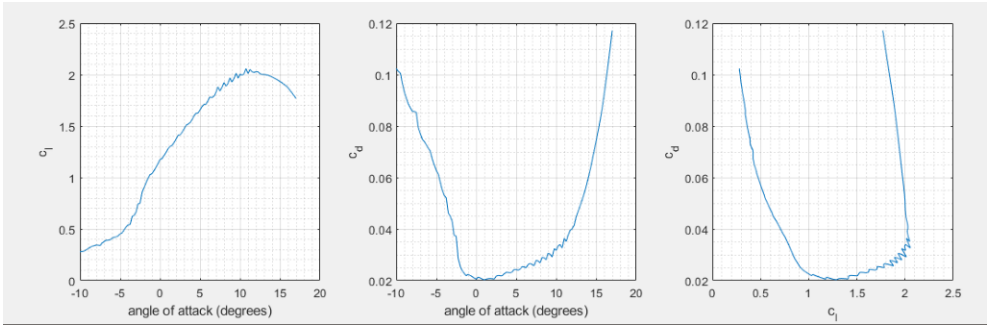

Figure 13: CH10 airfoil coefficients of lift and drag data plotted [7]

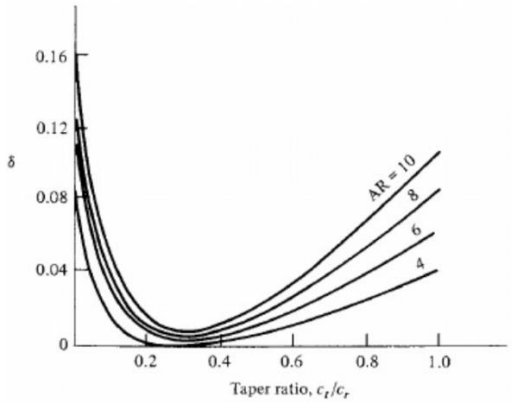

Figure 14: δ as a function of taper ratio for different AR [6]

Appendix B – Payload Prediction

The purpose of the payload prediction is for the team to observe what payloads are appropriate at specific altitudes. In order to produce the payload curve in Figure 15 seen below, the team began with analyzing lift performance data and linearizing it with altitude. Several variables were factored into this curve beginning with the idea that for a plane to carry a certain load, it would have to produce a far greater lift than its own weight to maintain flight. The density of air is another characteristic which is dependent of the altitude, this was kept in mind and compensated for. In Section 6.2.3, Figure 6 presents net thrust and lift plotted against velocity. From this, a max velocity is found where net thrust is zero. The maximum velocity also indicated the point of maximum lift, this was done at sixteen different altitudes as the air density varied. The weight of the empty aircraft was then subtracted from each of the maximum lifts found to give the following payload prediction at differing altitudes.

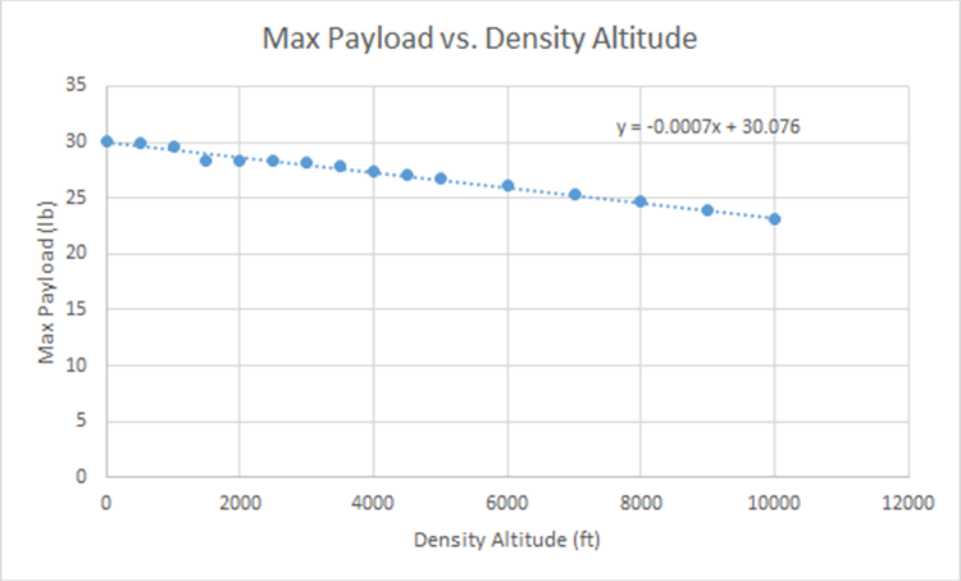

Figure 15: Payload Prediction Curve

Drawing 11X17

SUMMARY DATA	
WINGSPAN	120 IN
EMPTY WEIGHT	15.81LB
BATTERY CAPACITY	6s LIPO 5000 MAH
MOTOR	NEUMOTORS 4625 KV400
PROPELLER	TCF 18X8IN
SERVO	HITEC HS-5625MG TORQUE: 130.53 OZ-IN

	STABILITY MARGIN (IN)	X-DIRECTION CG FROM DATUM A (IN)
UNLOADED	22.37-27.34	26.49
LOADED	22.37-27.34	26.38

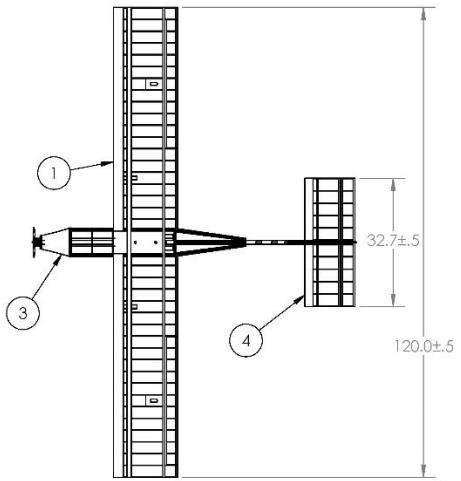

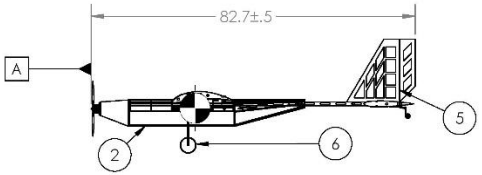

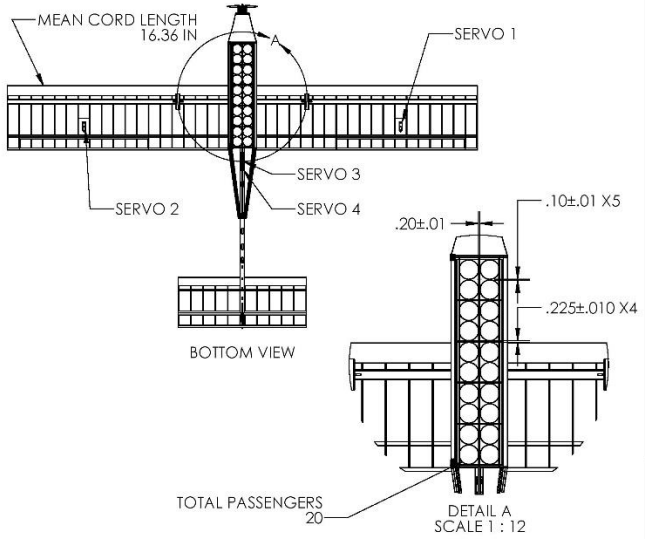

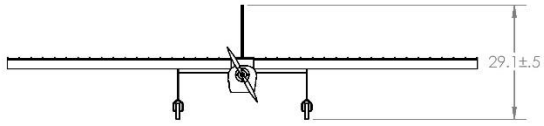

WEIGHT AND BALANCE			
ITEM	X DISTANCE FROM DATUM A (IN)	WEIGHT (LB)	RESULTANT MOMENT (LB*IN^2)
MOTOR	1.50	0.20	0.10
BATTERY	5.93	1.90	1.43
ESC	7.63	0.20	0.03
RECIEVER	8.30	0.02	0.001
SERVO 1	31.05	0.15	0.04
SERVO 2	31.05	0.15	0.04
SERVO 3	38.91	0.15	0.04
SERVO 4	41.26	0.15	0.04
PAYLOAD	26.63	12.48	33.19

SUBASSEMBLIES	
ITEM	BALLOON NUM.
MAIN WING	1
FUSELAGE	2
NOSE	3
HORIZ STABILIZER	4
VERTICAL STABILIZER	5
LANDING GEAR	6

UNLESS OTHERWISE SPECIFIED:
DIMENSIONS ARE IN INCHES
TOLERANCES:
FRACTIONAL± 0.5
MATERIAL
BALSA WOOD
BASSWOOD
ALUMINUM
DO NOT SCALE DRAWING

	NAME	DATE
DRAWN	JAMES S.	2/24/19
CHECKED		
ENG APPR.		
MFG APPR.		
Q.A.		
COMMENTS:		

NORHTERN ARIZONA UNIVERSITY

TITLE:
TEAM 45:
SKYJACKS

SIZE B | DWG. NO. FINAL DESIGN | REV 1

SCALE: 1:24 | WEIGHT: 28.29 LB | SHEET 1 OF 1